



# Loss of a Centrosomal Protein, Centlein, Promotes Cell Cycle Progression\*

YANG Ling, ZHANG Ying, YUAN Li\*\*

(Savaid School of Medicine, University of Chinese Academy of Sciences, Beijing 100049, China)

**Abstract** The centrosome is the principal microtubule organizing center in most animal cells. It ensures orderly cell cycle progression with accurate chromosome segregation. We have previously reported that the centrosomal protein Centlein functions as a molecular linker between C-Nap1 and Cep68 to maintain centrosome cohesion. To explore novel function of Centlein, in this study, we generated Centlein knockout cell lines, and performed RNA-seq and data analysis on Centlein knock out and control cells, in parallel. Ablation of Centlein upregulated *PLK1*, *CCNB1*, *CCNA2* and *CDC20*, and promoted cell cycle progression. PLK1 protein, found elevated in Centlein knock out cells, interacted with Centlein *in vivo*. We propose that centrosomal PLK1 exerting control over the cell cycle relies upon the interaction with Centlein.

**Key words** Centlein, RNA-seq, PLK1, centrosome, cell cycle progression

**DOI:** 10.16476/j.pibb.2019.0092

## 1 Introduction

In most cells, the centrosome serves as the major microtubule(MT) organizing center (MTOC)<sup>[1]</sup>, which coordinates most MT-related processes, including cell shape, polarity, adhesion and motility, cell division and cytokinesis, as well as intracellular transport<sup>[2-3]</sup>. In addition, the core centrosomal components, the centrioles, can function as basal bodies that seed the growth of cilia and flagella<sup>[4-5]</sup>. Aberrant centrosome function forms the etiologic basis for a growing number of human diseases<sup>[6-7]</sup>.

The mammalian centrosome is comprised of two centrioles(hereafter termed parental centrioles) and the surrounding pericentriolar material(PCM)<sup>[7]</sup>. The two centrioles within a G1 centrosome are ostensibly connected through a proteinaceous linker, often referred as centrosome cohesion<sup>[8]</sup>, intercentrosomal/centrosomal linker<sup>[9-10]</sup> or G1-G2 tether, emanating from their proximal ends. As cells progress from G1 into G2 phase, the centrosome is duplicated, and the duplicated centrosomes remain linked until late G2 phase to function as a single MTOC<sup>[11]</sup>. At the onset of mitosis, the intercentrosomal linker is disassembled *via* different mechanisms, coincident with centrosome separation in preparation for mitotic spindle

assembly<sup>[12-16]</sup>. For example, linker proteins C-Nap1 and Rootletin dissociate from mitotic centrosomes in response to phosphorylation by the Nek2A kinase<sup>[17-19]</sup> that is regulated by polo-like kinase1(PLK1), an important mitotic kinase that regulates centrosome maturation, including the recruitment of  $\gamma$ -tubulin and other centrosome components at G2/M<sup>[20-22]</sup>.

We have reported that Centlein, as a novel microtubule-associated protein, is involved in neurite formation<sup>[23]</sup> and required for centrosome cohesion<sup>[24]</sup>. To gain further insights into the cellular function of Centlein, we used the CRISPR(clustered regularly interspaced short palindromic repeat)-Cas9 system of RNA-guided endonuclease activity to disrupt the sequence coding for Centlein in hTERT-immortalized retinal pigment epithelial cells(RPE1). The transcriptome of Centlein-null and control cells were subjected to whole genome RNA sequencing(RNA-seq) analysis. We show here absence of Centlein upregulates *PLK1*, *CCNB1*, *CCNA2* and *CDC20*, and

\* This work was supported by a grant from The National Natural Science Foundation of China (31271522).

\*\* Corresponding author.

Tel: 86-10-88256717, E-mail: yuanli@mails.ucas.ac.cn

Received: April 28, 2019 Accepted: May 8, 2019

promotes cell cycle progression. Furthermore, we identified Centlein as a novel PLK1-binding protein.

## 2 Materials and methods

### 2.1 Materials

Precision Plus Protein Dual Color Standards was purchased from Bio-Rad; Lipofectamine 2000 reagent was purchased from Invitrogen; EDTA-free protease inhibitor cocktail was purchased from Roche; protein-G-Sepharose was purchased from Cowin Biotech; Dynabeads Protein G, ECL were purchased from GE Healthcare Life Sciences; Dulbecco's modified Eagle's medium DMEM and DME/F12 were purchased from Hyclone; RNAsimple total RNA kit was purchased from TIANGEN; reverse transcription kit was purchased from Promega; qRT-PCR reagent was purchased from Roche.

### 2.2 Cell culture and transfection

HeLa, HEK293T and RPE1 cells were cultured in Dulbecco's modified Eagle's medium(DMEM), DMEM and DME/F12 (1 : 1) respectively, and supplemented with 10% (v/v) fetal bovine serum (Hyclone), 100 IU/ml penicillin and 100 mg/L streptomycin. The cells were grown at 37°C in 5% CO<sub>2</sub>. HEK293T cells were transfected using Lipofectamine 2000 reagent, according to the manufacturer's protocol. Cells were collected to analyze 24 h after transfection.

### 2.3 RNA isolation and library construction

Cells were harvested to extract total RNA with TRIzol according to the standard protocol of RNAsimple Total RNA Kit. Agarose gel electrophoresis was performed to analyse RNA degradation and contamination. Total RNA samples, were sent to Anoroad(Beijing, Co. Ltd.) for whole transcriptome sequence. RNA purity was measured by NanoDrop 2000 spectrophotometer, concentration and quality were measured by Agilent 2100 Bioanalyzer and Agilent RNA 6000 Nano Kit respectively. cDNA was synthesized from the total RNA according to the standard protocol of Illumina Inc. The transcriptome was sequenced using Illumina HiSeq2500(Illumina, California, USA), mapping reads length PE150.

### 2.4 RNA-seq data analysis

The raw RNA-seq reads were cleaned by Trim Galore, removing low quality reads and reads

containing adapter sequence. The clean reads were aligned to Ensembl human genome GRCh37 using HISAT2<sup>[25]</sup>, then StringTie<sup>[26-27]</sup> was used for transcriptome re-assemble and gene quantification. Reference genome and annotations were both obtained from GENCODE(v19) project(<https://www.gencodegenes.org>). Normalized gene expression levels (measured by Fragments per Kilobase Million, FPKM) were used in following expression-related analysis.

### 2.5 DEGs identification and ontology enrichment

For the analysis of differentially expressed genes (DEGs), the raw read counts calculated from StringTie results were used as input data for DESeq2<sup>[28]</sup>. The estimated read count data was normalized using the shrinkage of effect size(LFC estimates) method, and the differential expression analysis between WT and D1 samples were performed with negative binomial GLM model in DESeq2 packages. DEGs with adjusted *P* value less than 0.05 and fold change greater than 10 were set as threshold for confident DEGs. Gene ontology analysis and enrichment of KEGG pathway were both performed on Enrichr<sup>[29-30]</sup> with an adjusted *P*-value cut-off of 0.05, and network of enriched KEGG pathway were plotted by R package igraph.

### 2.6 qRT-PCR analysis

The cDNA was reverse-transcribed from 2 µg of total RNA using MMLV(Moloney Murine Leukemia Virus) reverse transcriptase. Primer pairs were designed and blasted in national center for biotechnology information(NCBI), and synthesized by Tsingke Company(Beijing, China). The house keeping gene β-actin was considered as the control gene for normalization. Gene-specific mRNA levels were assessed by qRT-PCR using the SYBR Green kit on a LightCycler 480 instrument(Roche), with a 96-well plate was used to conduct the reaction. 10 µl Roche mix, 1 µl cDNA, 0.5 µl forward and 0.5 µl reverse primer, 8 µl double distilled water. Reaction procedure was as follow, 94°C 20 s, 58°C 20 s, 72°C 30 s, total 45 cycles, followed by pre-denaturation at 94°C 10 min. All analysis were repeated three times using biological replicates. The 2<sup>-ΔΔC<sub>t</sub></sup> method<sup>[31]</sup> was used to calculate relative gene expression level. Primer pairs were listed in Table 1.

**Table 1 Primers used in qRT-PCR**

Name	Sequence (5'-3')	Product length (bp)
PLK1-F	TTCGTGTTTCGTGGTGTGGA	117
PLK1-R	GCCAAGCACAAATTTGCCGTA	
CDC20-F	CCGAAGTCTGGCAAATCCA	81
CDC20-R	CTGCGATGGGGGATATAGCG	
CCNB1-F	GCAGCAGGAGCTTTTTGCTT	93
CCNB1-R	CCAGGTGCTGCATAACTGGA	
CCNA2-F	TGGTGGTCTGTGTCTGTGA	148
CCNA2-R	TGCCAGTCTTACTCATAGCTGA	
$\beta$ -actin F	TGACGTGGACATCCGCAAAG	205
$\beta$ -actin R	CTGGAAGGTGGACAGCGAAA	

## 2.7 Immunofluorescence microscopy, immunoprecipitation and immunoblotting

Procedure and equipment device were described elsewhere<sup>[24]</sup>, primary antibody used were mouse anti-Centlein(1 : 500, 11A4), rabbit anti-C-Nap1(1 : 800, 14498-1-AP, Proteintech), the secondary fluorescence antibody used were Alexa Fluor 488 goat anti-mouse IgG(1 : 1 000, A11029, Invitrogen), Alexa Fluor 594 goat anti-rabbit IgG(1 : 1 000, A11012, Invitrogen) for immunofluorescence microscopy, DAPI in ProLong Gold(Invitrogen, P36931). For immunoprecipitation and immunoblotting, antibody used were rabbit anti-PLK1(1 : 2 000, BS7198, Bioworld ), mouse anti-Centlein(1 : 1 000, 11A4), mouse anti-Myc (1 : 8 000, M047-3, MBL International), rabbit anti-GFP (1 : 1 000, 50430-2-AP, Proteintech), rabbit anti-GAPDH (1 : 2 000, B1034, Biodragon), mouse anti- $\beta$ -actin (1 : 5 000, M20010, Abmart). The secondary antibodies used were horseradish peroxidase(HRP) -conjugated goat anti-mouse IgG (1 : 8 000 GAM0072, Liankebio), HRP-conjugated goat anti-rabbit IgG (1 : 5 000, A0208, Beyotime).

## 2.8 FACS analysis

Cells were cultured on cell culture dish and were harvested by trypsinization, washed with phosphate-buffered saline and fixed in cold 70% ethanol overnight. After fixation, cells were incubated with staining buffer(100 g/L RNaseA and with 50 g/L propidium iodide, 0.2% TritonX-100) for 30 min at room temperature in dark place. Flow cytometry was carried using Accuri C6 flow cytometer(BD Biosciences), data was subjected to Flowjo7.6 for analyzing.

## 3 Results and discussion

### 3.1 Generation of RPE1 Centlein knockout cell lines

We have reported that Centlein is a novel NIMA related kinase 2(Nek2A) substrate<sup>[24]</sup>, and localized to the proximal ends of the centrioles<sup>[24]</sup>. Depletion of Centlein impairs recruitment of Cep68 to the centrosomes, in turn, results in premature centrosome separation in interphase cells, also called centrosome splitting<sup>[24,32]</sup>. Thus, centrosome cohesion is maintained by Centlein complexed with C-Nap1 and Cep68 to ensure the interphase centrosome(s) functioning as a single microtubule-organizing center.

For further insight into the cellular function of Centlein, we used CRISPR/Cas9-mediated gene-editing in RPE1 cell line to ablate Centlein. RPE-1 cells were chosen because they are nontransformed, chromosomally stable diploid cell chromosomally stable, and routinely used in the mitosis field to represent normal cells as a normal diploid cell line<sup>[33]</sup>. Immunoblot and immunofluorescence microscopy screening identified a Centlein-deficient clone(Figure 1c, d), and DNA sequence analysis confirmed a biallelic insertion of A that led to premature stop codons in the Centlein coding sequence(Figure 1a, b). This null clone(D1) was used for our analysis.

### 3.2 Exploration of the pathways affected by Centlein knockout using RNA-seq

We explored novel function of Centlein by performing RNA-seq technology to analyze the transcriptomic profile response in the absence of Centlein. We obtained 41.8 G data from these sequence libraries. Each library generated more than 45.6 million raw reads. Raw data was then filtered, removing adaptor(reads containing adaptor greater than 5 bp) and low quality sequences(in which reads more than 50% bases  $Q \leq 19$ ), and reads containing  $N > 5\%$ . The analysis of base composition and quality showed that the Q30 ratio(quality of bases  $\geq 30$ ) was 92.49%, indicate reliable base calling. The GC content of each sample ranged from 79.15% to 85.28% (Table 2).

To assess the effect of Centlein knockout, the Spearman correlation coefficients of global gene expression for each sample was constructed(Figure 2a). The hierarchical clustering results showed that samples from control and Centlein knockout groups

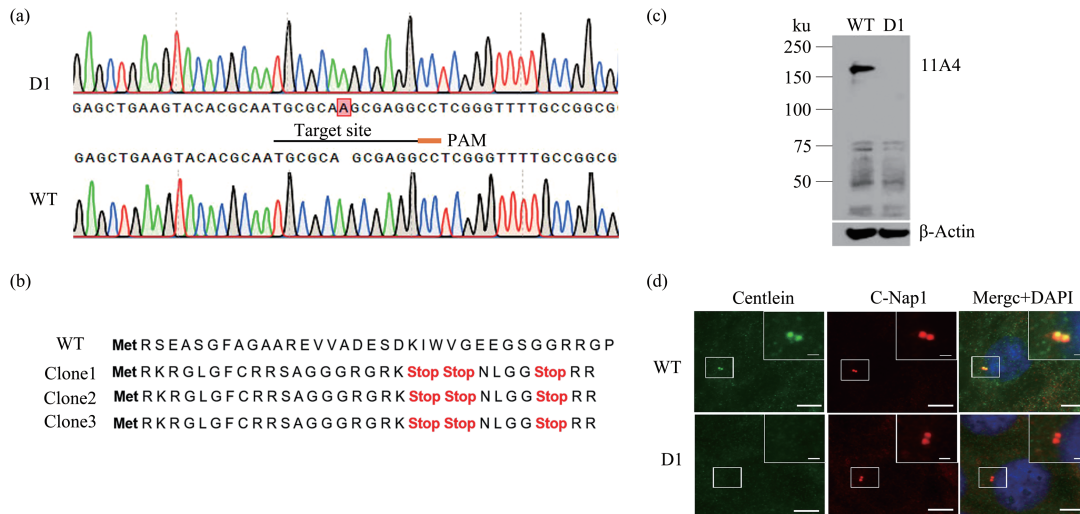


**Fig. 1** Generation of Centlein knock-out cell line

(a) Schematic represents the designed target site, sequence peak map displays single Adenine insertion in exon1, PCR was performed on genomic DNA from candidate clone D1, PCR products were recloned and sequenced, all sequence from clone D1 were identical, indicating biallelic intersion. (b) Exon1 translation analysis of WT and clones from D1. (c) Western blotting analysis of the WT, Centlein knock-out cell clone (D1) using mouse anti-Centlein antibody 11A4, using  $\beta$ -actin as loading control. (d) Cells were co-stained with the antibodies against Centlein (green) and C-Nap1 (red). DAPI was used to stain the nuclei (blue). The insets show enlarged views of centrosomes. Scale bars: 10  $\mu$ m; 1  $\mu$ m (insets).

**Table 2** General statistics of sequence data

Sample	Read length	Raw reads	Clean reads	Mapped reads	Mapping rate (%)	GC content (%)
KD_1	150	44678912	44676450	37305756	83.5	83.5
KD_2	150	45061802	45048604	37401936	83.02	83.02
KD_3	150	45340722	45328240	37370360	82.44	82.44
CONT_1	150	45269392	45267240	36513256	80.66	80.66
CONT_2	150	47254582	47252356	37401936	79.15	79.15
CONT_3	150	46178126	46176878	39381615	85.28	85.28

segregated into separate clusters, with accordance to the experimental design. To further explore the difference of genes expression between WT and D1, the differential expression analysis was performed using DESeq2. We identified 5 475 genes with at least five-fold change and  $FDR < 0.001$  between two groups (Figure 2b), and 1 013 and 1 210 DEGs were significantly up-regulated and down-regulated respectively in the D1 group compared to the WT group.

To understand the biological functions of the DEGs, the gene ontology(GO) enrichment analysis was performed using all DEGs(Figure 2c). The mitotic nuclear division process and mitotic spindle assembly functions were significantly enriched, in accordance with cell proliferation and cell cycle

progression. Then, we mapped the DEGs to the KEGG pathway database, and the KEGG pathway network were built using Enrichr (Figure 2d).

A total number of 11 pathways were significantly enriched( $FDR < 0.05$ ), where most of DEGs were involved in the Steroid hormone biosynthesis pathway as well as ovarian steroidogenesis and FoxO signaling pathway(Table 3). What's more, we observed the enrichment of cell cycle pathway in those DEGs, which attracted our focus among these theoretical pathways based on previous studies related to Centlein.

### 3.3 Upregulation of *PLK1*, *CCNB1*, *CCNA2* and *CDC20*, and promotion of cell cycle progression in cells deficient of Centlein

During the cell cycle, centrosomes are duplicated

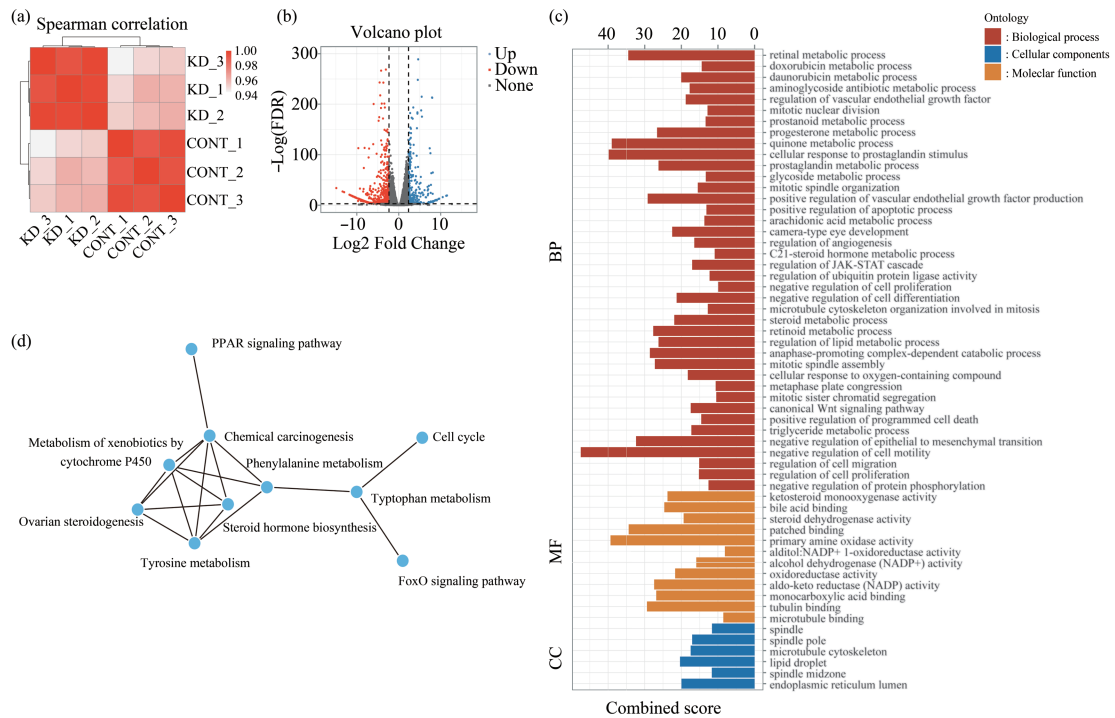


Fig. 2 RNA-seq analysis

(a) Spearman correlation of control and knockdown samples. The analysis was performed on genes expressed with at least 10 TPM in all samples. (b) Volcano plot of differentially expressed genes after Centlein knockout. Threshold for differential expression was set to at least 2-fold changes and at most 0.01 FDR. Genes that were significantly differentially expressed were colored in red and blue. (c) Gene Ontology enrichment analysis of differentially expressed genes. Horizontal axis represents the combined enrichment scores calculated from Enrichr. (d) Network of enriched KEGG pathways.

Table 3 KEGG pathway analysis

Term	ID	Overlap	FDR	Genes
Steroid hormone biosynthesis	hsa00140	6/58	0.000055	AKR1C1; HSD17B2; CYP1A1; AKR1C3; CYP1B1; AKR1C2
Ovarian steroidogenesis	hsa04913	5/50	0.000313	HSD17B2; CYP1A1; AKR1C3; CYP1B1; PTGS2
FoxO signaling pathway	hsa04068	6/133	0.001776	TGFB2; CCNB1; IL6; PLK1; FBXO32; SOD2
Chemical carcinogenesis	hsa05204	5/82	0.001776	ALDH1A3; CYP1A1; CYP1B1; AKR1C2; PTGS2
Cell cycle_Homo sapiens	hsa04110	5/124	0.007098	CDC20; CCNA2; TGFB2; CCNB1; PLK1
Phenylalanine metabolism	hsa00360	3/17	0.00196	AOC3; ALDH1A3; MAOA
PPAR signaling pathway	hsa03320	4/69	0.007098	FABP4; FABP5; ACSL5; PPARG
Metabolism of xenobiotics by cytochrome P450	hsa00982	4/73	0.007681	ALDH1A3; AKR1C1; CYP1A1; CYP1B1
Tyrosine metabolism	hsa00350	3/35	0.009816	AOC3; ALDH1A3; MAOA
Tryptophan metabolism	hsa00380	3/40	0.013097	MAOA; CYP1A1; CYP1B1
Oocyte meiosis	hsa04114	4/123	0.038528	CDC20; CCNB1; PLK1; AURKA

and segregated along with the genome. Emerging data suggest that centrosomes are essential for several cell cycle transitions, including the G1/S and G2/M transitions<sup>[34]</sup>. Given Centlein acting as a molecular link between C-Nap1 and Cep68 to maintain centrosome cohesion, we selected the genes annotated as belonging to the "cell cycle" category by KEGG

pathway for further assessment. qRT-PCR analysis confirmed significant upregulation of *PLK1*, *CCNB1*, *CCNA2* and *CDC20* in D1 cells(Figure 3). Then, Western blot analysis showed increase of *PLK1*, *CDC20*, *CCNA2*, *CCNB1* in D1 cells(Figure 4). *PLK1* plays pleiotropic roles in various essential cell-cycle related processes including centrosome

maturation, mitotic entry, checkpoint recovery, spindle assembly, sister chromatid separation, and cytokinesis<sup>[35]</sup>. Cyclin B, always complexes with cdk forming cyclinB-Cdk1 complex<sup>[36]</sup>, function as a vital regulator of mitotic entry and cell cycle progression. CyclinA2 is an essential regulator of the cell division cycle function through the activation of kinases which participate to the regulation of S phase as well as the mitotic entry, which was used as a marker for cell proliferation<sup>[37]</sup>. Cdc20 has important functions in chromosome segregation and mitotic exit<sup>[38]</sup>. The aforementioned quantitative PCR results promoted us to test whether cell cycle progression was altered. WT and D1 cells were subjected to flow cytometric

analysis of cell cycle profiles, in parallel. As shown in Figure 4, distribution of cell numbers in different phases was shown(Figure 5a, b), as statistical shown, the percentage of cells in S phase in the WT and D1 groups were (22.13±2.44)% and (23.03±2.39)% (Figure 5c), respectively. No significant difference was observed. However, the percentage of cells in S+G2/M phase was (29.53±2.23)% and (38.56±0.39)% (Figure 5c), respectively. Depletion of Centlein significantly increased the percentage of cells in S+G2/M phase(\**P*<0.01) (Figure 5d). Results above showed that ablation of Centlein remarkably promotes the cell cycle progression.

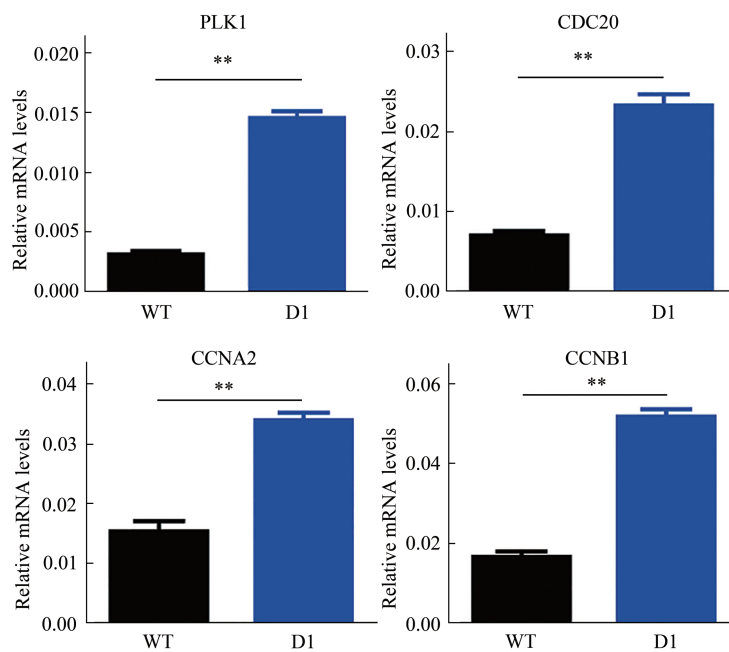


**Fig. 3** qRT-PCR validation of selected DEGs

RNA samples from biological replicates were subjected to qRT-PCR analysis, relative expression level was calculated by  $2^{-\Delta\Delta Ct}$  method, \*\**P*<0.01, mean±s.d..

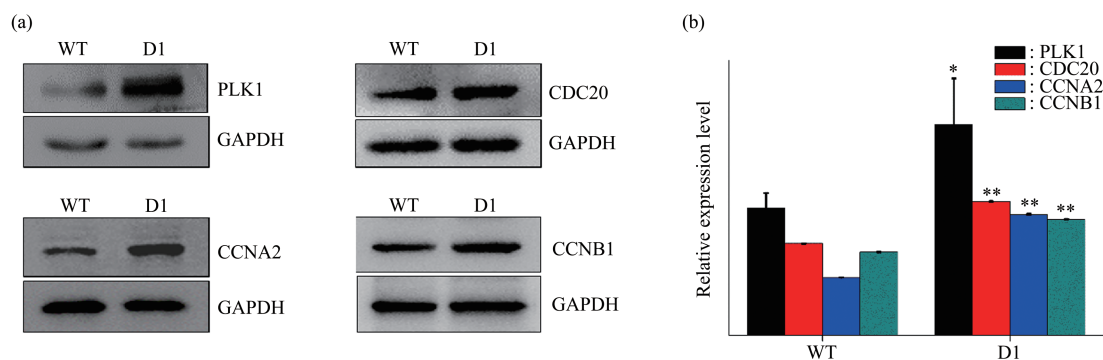


**Fig. 4** Examination of the protein level of PLK1, CDC20, CCNA2, CCNB1 in WT and D1

Western blot analysis of the upregulation of PLK1, CDC20, CCNA2, CCNB1, IntDen were measured by ImageJ, three biological replicates were used. \**P*<0.05, \*\**P*<0.01, mean±s.d..

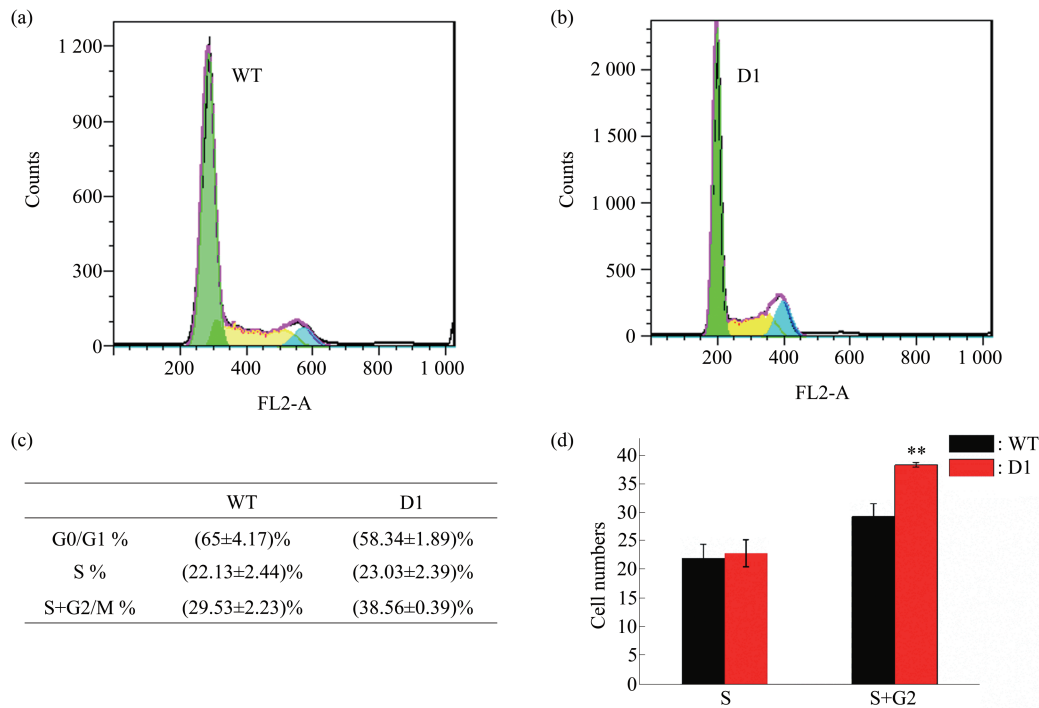


**Fig. 5 Depletion of Centlein promotes the cell cycle progression**

(a) The first green peak, the yellow portion in the middle and the blue peak represent G1 phase, S phase, G2/M phase respectively. (b) Cell distribution statu in D1 cell. (c) Summary statistical of percentage of cells in G0/G1, S and S+G2/M phase. (d) Quantitative of cell numbers in S phase and S+G2/M, \*\* $P < 0.01$ , mean±s.d..

### 3.4 Identification of PLK1 protein elevated in Centlein-KO cells as a novel binding partner of Centlein

FACS profiles, Western blotting and immunofluorescence microscopy have showed that PLK1 is targeted to centrosomes at the G1/S transition. Ablation of PLK1 significantly induces S-phase defects<sup>[39]</sup>, which are reversed by ectopic expression of PLK1, but not a mutant that fails to localize to centrosomes, demonstrating that centrosomal PLK1 is indispensable for S-phase progression.

Because of upregulation of *PLK1* in D1 cells, we wonder whether increased mRNA levels resulted in increased protein expression. Lysates from Centlein-null and control cells were analyzed by Western blotting with anti-PLK1 antibody(Figure 4a, left top), which showed that PLK1 protein levels were indeed increased in D1 cells(Figure 4b). Next, an interaction between Centlein and PLK1 was ascertained with reciprocal coimmunoprecipitation assays. The results revealed that endogenous Centlein coimmunoprecipitated with endogenous PLK1

(Figure 6a). Reversely, GFP-PLK1 could be co-immunoprecipitated after co-expression with Myc-Centlein(Figure 6b).

In summary, by RNA-seq and quantitative(real time) PCR analyses. we show here ablation of Centlein upregulates Plk1, cyclinB1, cyclinA2 and

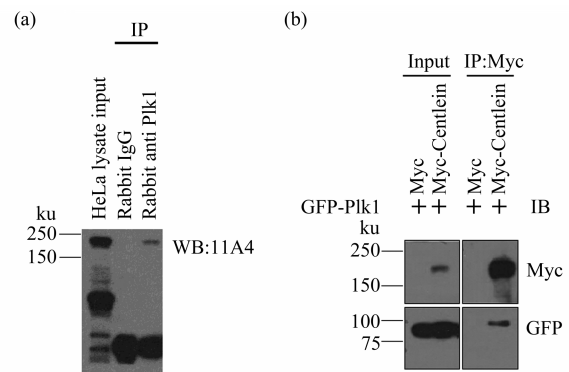


**Fig. 6 Centlein interacts with PLK1**

(a) Western blotting of endogenous Centlein with mouse anti-Centlein 11A4 after immunoprecipitation with an antibody against PLK1. (b) 293T cells was transfected with myc-Centlein and GFP-PLK1, immunoprecipitate with myc antibody and immunoblotted with antibody against GFP.

Cdc20. Elevated PLK1 protein in Centlein-KO cells may account for accelerated cell cycle progression. In addition, we identified Centlein as a novel binding partner of PLK1. In light of this, we hypothesize that Centlein ablation may affect centrosomal localization of PLK1. Accumulating data suggest that there may be mutual communications between centrosome(s) and the nucleus to coordinate both centrosome and DNA events throughout the entire cell cycle<sup>[40]</sup>. Several DNA replication factors, including geminin, origin recognition complex(ORC) and minichromosome maintenance(MCM) proteins, localize to centrosomes and play crucial roles in the centrosome cycle<sup>[40]</sup>. Some ORC, MCM, cyclin E cyclin A not only colocalize with PLK1 at centrosomes, but also interact with PLK1<sup>[40-43]</sup>. Previous studies have implied an important role for centrosomes in the G1/S and G2/M transitions<sup>[7,34]</sup>. Aberrant expression of *PLK1*, *CDC20*, *CCNA2* and *CCNB1* has been identified closely related to various cancers<sup>[44-56]</sup>. Therefore, further studies will be conducted to elucidate the functional relationship between Centlein and centrosomal PLK1.

**Acknowledgments** We thank ZHANG Jin-Yang and DU Bao-Zhen (Beijing Institutes of Life Science) for kindly providing assistance in RNA-seq analysis.

### References

- [1] Bornens M. Centrosome composition and microtubule anchoring mechanisms. *Curr Opin Cell Biol*, 2002, **14**(1): 25-34
- [2] Schatten H. The mammalian centrosome and its functional significance. *Histochem Cell Biol*, 2008, **129**(6): 667-686
- [3] Khodjakov A, Rieder C L. Centrosomes enhance the fidelity of cytokinesis in vertebrates and are required for cell cycle progression. *J Cell Biol*, 2001, **153**(1): 237-242
- [4] Kobayashi T, Dynlacht B D. Regulating the transition from centriole to basal body. *J Cell Biol*, 2011, **193**(3): 435-444
- [5] Pedersen L B, Veland I R, Schroder J M, *et al.* Assembly of primary cilia. *Dev Dyn*, 2008, **237**(8): 1993-2006
- [6] Badano J L, Teslovich T M, Katsanis N. The centrosome in human genetic disease. *Nat Rev Genet*, 2005, **6**(3): 194-205
- [7] Nigg E A, Raff J W. Centrioles, centrosomes, and cilia in health and disease. *Cell*, 2009, **139**(4): 663-678
- [8] Barrera J A, Kao L R, Hammer R E, *et al.* CDK5RAP2 regulates centriole engagement and cohesion in mice. *Dev Cell*, 2010, **18**(6): 913-926
- [9] Bornens M, Paintrand M, Berges J, *et al.* Structural and chemical characterization of isolated centrosomes. *Cell Motil Cytoskeleton*, 1987, **8**(3): 238-249
- [10] Mardin B R, Schiebel E. Breaking the ties that bind: new advances in centrosome biology. *J Cell Biol*, 2012, **197**(1): 11-18
- [11] Nigg E A, Stearns T. The centrosome cycle: Centriole biogenesis, duplication and inherent asymmetries. *Nat Cell Biol*, 2011, **13**(10): 1154-1160
- [12] Jean C, Tollon Y, Raynaud-Messina B, *et al.* The mammalian interphase centrosome: two independent units maintained together by the dynamics of the microtubule cytoskeleton. *European Journal of Cell Biology*, 1999, **78**(8): 549-560
- [13] Bahmanyar S, Kaplan D D, Deluca J G, *et al.* beta-Catenin is a Nek2 substrate involved in centrosome separation. *Genes Dev*, 2008, **22**(1): 91-105
- [14] Barr F A, Sillje H H, Nigg E A. Polo-like kinases and the orchestration of cell division. *Nat Rev Mol Cell Biol*, 2004, **5**(6): 429-440
- [15] Yin H, Zheng L, Liu W, *et al.* Rootletin prevents Cep68 from VHL-mediated proteasomal degradation to maintain centrosome cohesion. *Biochim Biophys Acta Mol Cell Res*, 2017, **1864**(4): 645-654
- [16] Hardy T, Lee M, Hames R S, *et al.* Multisite phosphorylation of C-Nap1 releases it from Cep135 to trigger centrosome disjunction. *Journal of Cell Science*, 2014, **127**(Pt 11): 2493-2506
- [17] Fry A M, Mayor T, Meraldi P, *et al.* C-Nap1, a novel centrosomal coiled-coil protein and candidate substrate of the cell cycle-regulated protein kinase Nek2. *J Cell Biol*, 1998, **141**(7): 1563-1574
- [18] Mayor T, Stierhof Y D, Tanaka K, *et al.* The centrosomal protein C-Nap1 is required for cell cycle-regulated centrosome cohesion. *J Cell Biol*, 2000, **151**(4): 837-846
- [19] Faragher A J, Fry A M. Nek2A kinase stimulates centrosome disjunction and is required for formation of bipolar mitotic spindles. *Mol Biol Cell*, 2003, **14**(7): 2876-2889
- [20] Sdelci S, Schutz M, Pinyol R, *et al.* Nek9 phosphorylation of NEDD1/GCP-WD contributes to Plk1 control of gamma-tubulin recruitment to the mitotic centrosome. *Curr Biol*, 2012, **22**(16): 1516-1523
- [21] Wang G, Chen Q, Zhang X, *et al.* PCM1 recruits Plk1 to the pericentriolar matrix to promote primary cilia disassembly before mitotic entry. *Journal of Cell Science*, 2013, **126**(Pt 6): 1355-1365
- [22] Mardin B R, Agircan F G, Lange C, *et al.* Plk1 controls the Nek2A-PP1gamma antagonism in centrosome disjunction. *Curr Biol*, 2011, **21**(13): 1145-1151
- [23] Jing Z, Yin H, Wang P, *et al.* Centlein, a novel microtubule-associated protein stabilizing microtubules and involved in neurite formation. *Biochem Biophys Res Commun*, 2016, **472**(2): 360-365
- [24] Fang G, Zhang D, Yin H, *et al.* Centlein mediates an interaction between C-Nap1 and Cep68 to maintain centrosome cohesion. *Journal of Cell Science*, 2014, **127**(Pt 8): 1631-1639
- [25] Kim D, Langmead B, Salzberg S L. HISAT: a fast spliced aligner with low memory requirements. *Nat Methods*, 2015, **12**(4): 357-360

- 357-360
- [26] Pertea M, Pertea G M, Antonescu C M, *et al.* StringTie enables improved reconstruction of a transcriptome from RNA-seq reads. *Nat Biotechnol*, 2015, **33**(3): 290-295
- [27] Pertea M, Kim D, Pertea G M, *et al.* Transcript-level expression analysis of RNA-seq experiments with HISAT, StringTie and Ballgown. *Nat Protoc*, 2016, **11**(9): 1650-1667
- [28] Love M I, Huber W, Anders S. Moderated estimation of fold change and dispersion for RNA-seq data with DESeq2. *Genome Biol*, 2014, **15**(12): 550
- [29] Kuleshov M V, Jones M R, Rouillard A D, *et al.* Enrichr: a comprehensive gene set enrichment analysis web server 2016 update. *Nucleic Acids Res*, 2016, **44**(W1): W90-97
- [30] Chen E Y, Tan C M, Kou Y, *et al.* Enrichr: interactive and collaborative HTML5 gene list enrichment analysis tool. *BMC Bioinformatics*, 2013, **14**:128
- [31] Vandesompele J, De Preter K, Pattyn F, *et al.* Accurate normalization of real-time quantitative RT-PCR data by geometric averaging of multiple internal control genes. *Genome Biol*, 2002, **3**(7): Research0034
- [32] Meraldi P, Nigg E A. Centrosome cohesion is regulated by a balance of kinase and phosphatase activities. *Journal of Cell Science*, 2001, **114**(Pt 20): 3749-3757
- [33] Jiang X R, Jimenez G, Chang E, *et al.* Telomerase expression in human somatic cells does not induce changes associated with a transformed phenotype. *Nature Genetics*, 1999, **21**(1): 111-114
- [34] Doxsey S, Zimmerman W, Mikule K. Centrosome control of the cell cycle. *Trends Cell Biol*, 2005, **15**(6): 303-311
- [35] Colicino E G, Hehnl H. Regulating a key mitotic regulator, polo-like kinase 1 (PLK1). *Cytoskeleton (Hoboken, NJ)*, 2018, **75**(11): 481-494
- [36] Fisher D, Krasinska L, Coudreuse D, *et al.* Phosphorylation network dynamics in the control of cell cycle transitions. *J Cell Sci*, 2012, **125**(Pt 20): 4703-4711
- [37] Loukil A, Cheung C T, Bendris N, *et al.* Cyclin A2: At the crossroads of cell cycle and cell invasion. *World J Biol Chem*, 2015, **6**(4): 346-350
- [38] Kapanidou M, Curtis N L, Bolanos-Garcia V M. Cdc20: At the crossroads between chromosome segregation and mitotic exit. *Trends Biochem Sci*, 2017, **42**(3): 193-205
- [39] Shen M, Cai Y, Yang Y, *et al.* Centrosomal protein FOR20 is essential for S-phase progression by recruiting Plk1 to centrosomes. *Cell Res*, 2013, **23**(11): 1284-1295
- [40] Knockleby J, Lee H. Same partners, different dance: involvement of DNA replication proteins in centrosome regulation. *Cell Cycle (Georgetown, Tex)*, 2010, **9**(22): 4487-4491
- [41] Tsvetkov L, Stern D F. Interaction of chromatin-associated Plk1 and Mcm7. *The Journal of Biological Chemistry*, 2005, **280**(12): 11943-11947
- [42] Y M. A centrosomal localization signal in cyclin E required for Cdk2 -independent S phase entry. *Science*, 2004, **306**(5697): 885-888
- [43] Pascreau G, Eckerdt F, Churchill M E A, *et al.* Discovery of a distinct domain in cyclin A sufficient for centrosomal localization independently of Cdk binding. *Proc Natl Acad Sci USA*, 2010, **107**(7): 2932-2937
- [44] Tut T G, Lim S H, Dissanayake I U, *et al.* Upregulated Polo-like kinase 1 expression correlates with inferior survival outcomes in rectal cancer. *Plos One*, 2015, **10**(6): e0129313
- [45] Li Z, Liu J, Li J, *et al.* Polo-like kinase 1 (Plk1) overexpression enhances ionizing radiation-induced cancer formation in mice. *J Biol Chem*, 2017, **292**(42): 17461-17472
- [46] Karra H, Repo H, Ahonen I, *et al.* Cdc20 and securin overexpression predict short-term breast cancer survival. *Br J Cancer*, 2014, **110**(12): 2905-2913
- [47] Li J, Gao J Z, Du J L, *et al.* Increased CDC20 expression is associated with development and progression of hepatocellular carcinoma. *Int J Oncol*, 2014, **45**(4): 1547-1555
- [48] Gayyed M F, El-Maqsoud N M, Tawfik E R, *et al.* A comprehensive analysis of CDC20 overexpression in common malignant tumors from multiple organs: its correlation with tumor grade and stage. *Tumour Biol*, 2016, **37**(1): 749-762
- [49] Zhuang L, Yang Z, Meng Z. Upregulation of BUB1B, CCNB1, CDC7, CDC20, and MCM3 in tumor tissues predicted worse overall survival and disease-free survival in hepatocellular carcinoma patients. *Biomed Res Int*, 2018, **2018**: 7897346
- [50] Kim Y, Choi J W, Lee J H, *et al.* Spindle assembly checkpoint MAD2 and CDC20 overexpressions and cell-in-cell formation in gastric cancer and its precursor lesions. *Hum Pathol*, 2019, **85**:174-183
- [51] Mao Y, Li K, Lu L, *et al.* Overexpression of Cdc20 in clinically localized prostate cancer: relation to high Gleason score and biochemical recurrence after laparoscopic radical prostatectomy. *Cancer Biomark*, 2016, **16**(3): 351-358
- [52] Wang J, Zhou F, Li Y, *et al.* Cdc20 overexpression is involved in temozolomide-resistant glioma cells with epithelial-mesenchymal transition. *Cell Cycle*, 2017, **16**(24): 2355-2365
- [53] Wang S, Chen B, Zhu Z, *et al.* CDC20 overexpression leads to poor prognosis in solid tumors: A system review and meta-analysis. *Medicine (Baltimore)*, 2018, **97**(52): e13832
- [54] Shi R, Sun Q, Sun J, *et al.* Cell division cycle 20 overexpression predicts poor prognosis for patients with lung adenocarcinoma. *Tumour Biol*, 2017, **39**(3): 1010428317692233
- [55] Dong S, Huang F, Zhang H, *et al.* Overexpression of BUB1B, CCNA2, CDC20, and CDK1 in tumor tissues predicts poor survival in pancreatic ductal adenocarcinoma. *Biosci Rep*, 2019, **39**(2), pii: BSR20182306
- [56] Fang Y, Yu H, Liang X, *et al.* Chk1-induced CCNB1 overexpression promotes cell proliferation and tumor growth in human colorectal cancer. *Cancer Biol Ther*, 2014, **15**(9): 1268-1279

# 中心体蛋白Centlein的敲除促进细胞周期进程\*

杨岭 张莹 袁莉\*\*

(中国科学院大学存济医学院, 北京 100049)

**摘要** 中心体是大部分动物细胞的微管组织中心, 它确保了有序的细胞周期进程以及染色体的精确分离, 我们之前报道了中心体蛋白Centlein作为一个分子连接, 与C-Nap1和Cep68一起形成复合物维持中心体的连接. 然而, 关于Centlein的其他功能我们还知之甚少. 在本研究中, 建立了Centlein的敲除细胞系, 并且运用RNA-seq技术分析了敲除细胞系和正常野生型细胞系之间转录水平的差异. 发现Centlein敲除细胞系中细胞周期相关基因*PLK1*、*CCNB1*、*CCNA2*和*CDC20*的表达量上调, 流式结果又表明Centlein的敲除促进了细胞周期进程. 同时发现Centlein与PLK1之间存在细胞内相互作用, 于是我们提出了Centlein通过与PLK1的作用参与细胞周期进程.

**关键词** Centlein, RNA-seq, PLK1, 中心体, 细胞周期

**中图分类号** Q2, Q7

**DOI:** 10.16476/j.pibb.2019.0092

\* 国家自然科学基金(31271522)资助项目.

\*\* 通讯作者. Tel:010-88256717, E-mail:yuanli@mailsucas.ac.cn

收稿日期: 2019-04-28, 接受日期: 2019-05-08